Isocyanate-modified TiO$_2$ visible-light-activated photocatalyst

Dong Jiang [a,b], Yao Xu [a,*], Dong Wu [a], Yuhan Sun [a,*]

[a] State Key Laboratory of Coal Conversion, Institute of Coal Chemistry, Chinese Academy of Sciences, Taiyuan 030001, PR China
[b] Graduate University of the Chinese Academy of Sciences, Beijing 100049, PR China

ARTICLE INFO

ABSTRACT

Visible-activated TiO$_2$ photocatalysts were prepared by surface modification to TiO$_2$ with different isocyanates, including conjugated structured Tolylene-2,4-diisocyanate (TDI) and unconjugated structured m-Xylylene diisocyanate (m-XDI). These two isocyanates could be anchored on the TiO$_2$ surface via π-conjugated chemical bonds of –NHCOOTi, which were formed through the reaction between –NCO groups of isocyanates and the hydroxyl groups of TiO$_2$, and confirmed by FT-IR, XPS and UV–Vis spectra. As a result, donor–acceptor type π-conjugated systems came into being between isocyanate and TiO$_2$. Because the TDI molecules were conjugated themselves, perfect π-conjugated systems were produced in TDI-modified TiO$_2$ samples. Nevertheless, m-XDI-modified TiO$_2$ samples showed poor π-conjugation due to the lack of conjugation of m-XDI. Therefore, TDI-modified TiO$_2$ materials exhibited stronger visible absorption than m-XDI-modified TiO$_2$ in the range from 400 to 600 nm. Methylene blue, as a photodegradation target, was used to evaluate the photocatalytic performance, TDI-modified TiO$_2$ materials exhibited higher photocatalytic activity than m-XDI-modified TiO$_2$ and unmodified TiO$_2$. Moreover, the higher dosage of isocyanate would lead to the better photocatalytic activity.

© 2008 Elsevier B.V. All rights reserved.

1. Introduction

Since the discovery of photoelectrochemical splitting of water on n-TiO$_2$ electrodes in 1972 [1], titania-mediated heterogeneous photocatalysts have attracted extensive interest because of the potential applications in hydrogen production and environment protection. Nanocrystalline TiO$_2$ as a photocatalyst has a great many advantages such as low-cost, nontoxicity, high catalysis efficiency, long-term stability, energy-saving, etc., and becomes a very promising material for photocatalytic degradation of water pollutants [2,3]. However, the widespread technological application of TiO$_2$ photocatalysts are hampered by its band gap (3.2 eV for anatase TiO$_2$) and the requirement of ultraviolet radiation ($\lambda \leq 380$ nm) for photocatalytic activation. The sun can provide an abundant source of photons, but UV light accounts for only a small fraction ($\sim 5\%$) of the sun's energy compared with visible light (45%). Thus, recent efforts have been focused on exploring methods to utilize the inexhaustible sunlight and shift the TiO$_2$ photocatalytic response to the visible region.

In earlier investigations, the lattice Ti ion was replaced by various transition-metal ions including V, Mn, Cr, Au, Pt, Fe and Co ions [4–13], and in a few cases the resultant materials were active under visible light irradiation. However, these metal-doped TiO$_2$ materials suffered from poor thermal stability and increased carrier-recombination. Later, it was found that doping or modification with nonmetals such as carbon [14,15], nitrogen [16–24], sulfur [25,26], fluorine [27] and boron [28] also made TiO$_2$ show visible photocatalytic activity. Particularly, nitrogen-doped and carbon-doped TiO$_2$ materials have received much attention since Asahi [16] and Khan [14] et al. reported the visible photocatalytic activity of these materials. Unfortunately, the above-mentioned inorganic-modified TiO$_2$ (metal and nonmetal doping TiO$_2$) could not adequately utilize visible light due to their poor visible absorption. Lately, organic modification to TiO$_2$ was also proved to be efficient to endow TiO$_2$ with visible photocatalytic capability, and much attention has been paid to dye-sensitized TiO$_2$ materials that showed photocatalytic activity under visible light [31–33]. However, for the dye-sensitized TiO$_2$ photocatalyst, the dye molecules were only adsorbed on the TiO$_2$ surface and no steady chemical bond was formed between TiO$_2$ and the dye molecules. The dye molecules as a sensitizer easily desorbed to result in the decrease of photocatalytic activity during the reaction process. To overcome this difficulty, another route to organic modification to TiO$_2$ was realized by a chemical reaction between TiO$_2$ and organic compounds having phenolic hydroxyls, such as catechol [34,35], salicylic [36] and binaphthol [37]. But, due to the weak reactivity of these organic

* Corresponding authors. Tel.: +86 351 4049859; fax: +86 351 4041153.
E-mail addresses: xuyao@sxicc.ac.cn (Y. Xu), yhsun@sxicc.ac.cn (Y. Sun).
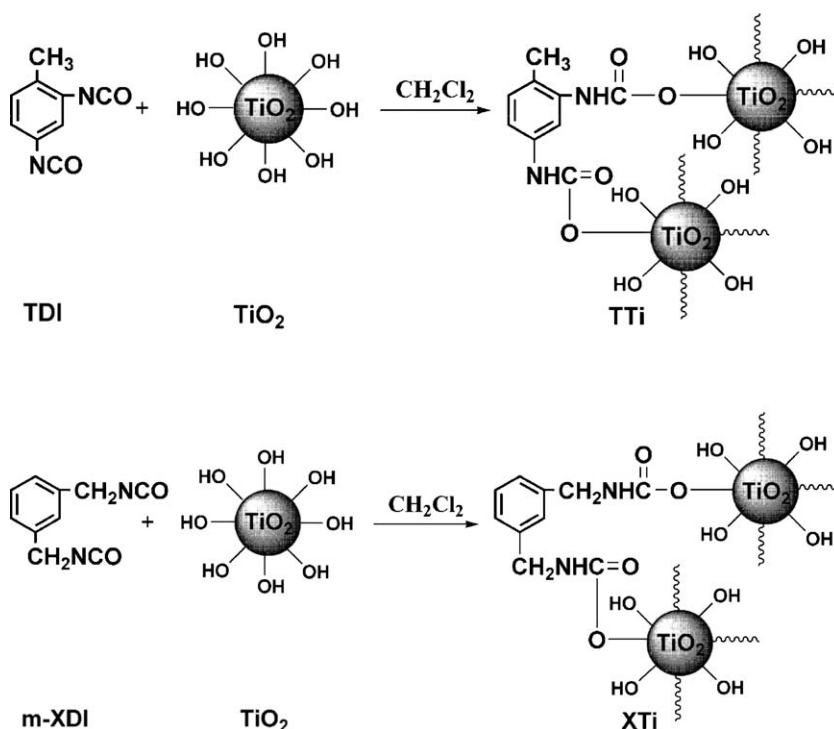
Scheme 1. Schematic illustrations of the formation process of TTi and XTi sample.

compounds, the reactions generally require long time to complete. Therefore, it is necessary to explore a new synthetic strategy to prepare visible-light-activated TiO₂ photocatalyst to avoid the problem encountered in previous routes.

In our previous communication, it was proved that Tolylene-2,4-diisocyanate (TDI) and dye modification to TiO₂ could make TiO₂ show visible absorption and exhibit good visible photocatalytic activity [38,39]. In the present paper, Tolylene-2,4-diisocyanate as a conjugated structured isocyanate and m-Xylylene diisocyanate (m-XDI) as an unconjugated structured isocyanate were representatively chosen to modify the original TiO₂. Herein, we will systematically discuss the preparation, characterization and photocatalytic activity of two different isocyanate-modified TiO₂ and the effect of isocyanate molecular structure on the property of final products.

2. Experimental methods

2.1. Synthesis of samples

In the present work, all chemical reagents were used without further purification. Original TiO₂ powders were prepared by a sol–gel-hydrothermal method [40], using titanium n-butoxide (TB) (CP, Shanghai Regent Company) and nitric acid (HNO₃) (AP, Taiyuan Chemical Engineering Factory) as the starting materials. 17 mL of TB was added dropwise to 50 mL of 2 M HNO₃ with magnetic stirring for 30 min to form a clear yellowish sol. Then the sol was transferred into a Teflon-line stainless steal autoclave to be hydrothermally treated at 140 °C for 12 h. After being naturally cooled to room temperature, the resulting precipitate was filtrated and washed three times with distilled water. The product was dried at 100 °C and ground into white powder.

In a typical surface modification procedure, 0.01 mol of as-prepared TiO₂ was dispersed in dichloromethane (CH₂Cl₂) (99.5%+, Beijing Reagent Company) under magnetic stirring and

produced a white suspension. Then 0.002 mol of Tolylene-2,4-diisocyanate (99.5%+, Aldrich) was added dropwise into the above suspension under nitrogen and the system turned to deeply yellow, suggesting that a chemical reaction occurred between the TDI molecules and TiO₂. The reaction is schematically shown in Scheme 1. The formed CH₂Cl₂ suspension was stirred at room temperature for 2 h, filtered and washed three times with CH₂Cl₂ to eliminate the adsorption of TDI on the TiO₂ surface. The final product was dried at 60 °C under vacuum and designated as TTi0.2 and TTi0.5 according to the different molar ratios of TDI/TiO₂ 0.2/1 and 0.5/1. The TDI-modified TiO₂ samples were called by a joint name: TTi samples. For comparative purpose, a reference experiment was carried out between m-Xylylene diisocyanate (m-XDI) (99.5%+, Aldrich) and TiO₂ (the m-XDI/TiO₂ molar ratio = 0.2/1 and 0.5/1) under the same reaction condition as above. The m-XDI-modified TiO₂ materials were assigned as XTi0.2 and XTi0.5 and called by a joint name: XTi samples. The structures of the TDI and m-XDI molecules are given in Fig. 1.

2.2. Characterization of samples

The crystalline phase of the samples was measured by X-ray diffraction (XRD, Cu Kα, 40 kV, 100 mA, D/max2500 Rigaku). The morphologies of samples were observed with a transmission electron microscope (TEM, Hitachi-600-2). The BET surface area was measured by nitrogen adsorption at 77 K (Tristar3000, Micromeritics). Chemical structure information of samples was collected using FT-IR spectra (Nicolet 470 Spectrometer) with 4 cm⁻¹ resolution. The surface element composition and the chemical state of the samples were determined by X-ray photoelectron spectroscopy (XPS, Mg Kα as radiation source, PHI-5300X, PerkinElmer Physics Electronics). UV–Vis diffuse reflectance spectra (DRS) and UV–Vis absorption spectra were recorded on a Shimadzu UV-3150 apparatus. The DRS system was equipped with an integrating sphere and used BaSO₄ as a reference.
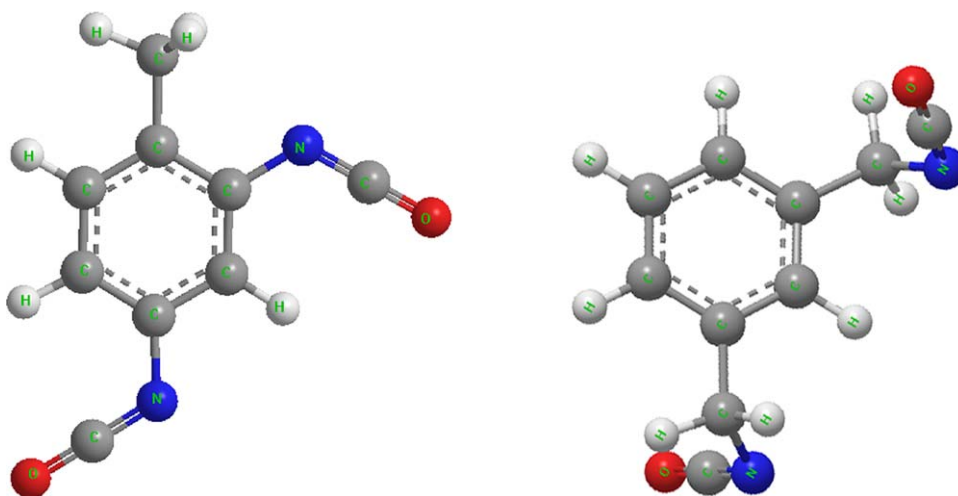
Fig. 1. The molecule structure of TDI (left) and m-XDI (right).

2.3. Photodegradation of methylene blue (MB)

The photocatalytic activities of unmodified TiO_2, TDI-modified TiO_2 samples, and m-XDI-modified TiO_2 samples were studied by measuring the degradation of methylene blue in aqueous solution under visible light irradiation. A 250-W metal halide lamp (Philips) was used as the light source and positioned inside a cylindrical Pyrex vessel surrounded by a circulating water jacket to cool the lamp. A cutoff filter was also placed outside the Pyrex jacket to remove radiation below 420 nm and completely ensure irradiation only by visible light wavelengths.

Aqueous photocatalyst dispersion was prepared by adding 250 mg of catalyst to a 250 mL solution containing MB at an appropriate concentration of 50 ppm. In all experiments, prior to irradiation, the suspension of catalyst in MB solution was stirred in the dark for 30 min to achieve an adsorption/desorption equilibrium. The concentration of MB at this point was used as the initial value for the further kinetic study of the photodegradation process. At given irradiation time intervals, the dispersion was sampled (4 mL), centrifuged, and subsequently filtered through a Millipore filter (pore size, 0.22 μm) to separate the catalyst particles. The filtrates were analyzed using UV–Vis spectra to determine the concentration of MB. The stability of the catalysts was investigated by the circular photodegradation experiments that were carried out under the same reaction condition as above-mentioned. Each time recycle finished, the used catalyst was centrifuged, washed with ethanol and dried before reuse. The recycling period was set to 14 h.

3. Results and discussion

3.1. Surface modification

Scheme 1 presents a schematic illustration of the formation of isocyanate-modified TiO_2 samples (TTi and XTi). In Scheme 1, it is observed that some free hydroxyls exist on the surface of pure TiO_2, and that each isocyanate (TDI and m-XDI) molecule possesses two active –NCO groups. The preparation of isocyanate-modified TiO_2 was carried out though the reaction between the Ti-OH groups of TiO_2 and –NCO groups of isocyanate. These surface Ti-OH hydroxyls could easily react with –NCO active groups to form the π-conjugated structure of –NHCOOTi. Hence, for the obtained TTi and XTi samples, isocyanate was anchored on the TiO_2 surface via the π-conjugated –NHCOOTi bond, not by

adsorption. Noticeable, there were wonderful π-conjugated surface complexes for the TTi samples because the TDI molecule was a conjugated structure itself (see Fig. 1), and XTi sample had partially π-conjugated surface complexes due to the lack of conjugation of m-XDI molecule itself (see Fig. 1). As a result, perfect π-conjugated and poor π-conjugated surface complexes were formed on the TiO_2 surface via the chemical bond of –NHCOOTi for the TTi and XTi samples, respectively. The formation of conjugated surface complexes will theoretically lead to the red-shift of the UV–Vis absorption [37,41]; however, the different conjugation degree between TTi and XTi samples would result in a different red-shifted absorption, which will be discussed in detail in the following section of UV–Vis spectra.

3.2. Crystal phase and morphography

The properties of TiO_2, TTi and XTi samples were listed in Table 1. In Table 1, it could be found that the unmodified TiO_2 and as-prepared TTi and XTi samples are all of the anatase crystal phase of TiO_2 without any other crystal phases. The same phase implied that isocyanate modification to TiO_2 had no effect on the crystalline phase of TiO_2. However, the surface areas of TTi and XTi samples were far less than that of unmodified TiO_2. After modification, surface area decreased gradually from 239.3 m^2/g of pure TiO_2 to 54.0 m^2/g of TTi0.5 and 58.3 m^2/g of XTi0.5 respectively, with the increasing content of isocyanate. Generally, the decrease in surface area was attributed to the aggregation between TiO_2 particles. About this point, TEM could give obvious supporting evidence. As shown in Fig. 2, the representative TEM images illustrated that unmodified TiO_2 appeared with less aggregation, but isocyanate-modified TiO_2 showed strong aggregation. Moreover, the aggregation extent increased with the rise of TDI/TiO_2 molar ratios for the TTi samples, to which the behavior of XTi samples was similar.

Table 1
The properties of samples.

Samples	Isocyanate/TiO_2 molar ratio	XRD structure	Surface area ($m^2\,g^{-1}$)
TiO_2	/	Anatase	239.3
TTi0.2	0.2	Anatase	91.9
TTi0.5	0.5	Anatase	54.0
XTi0.2	0.2	Anatase	95.6
XTi0.5	0.5	Anatase	58.3
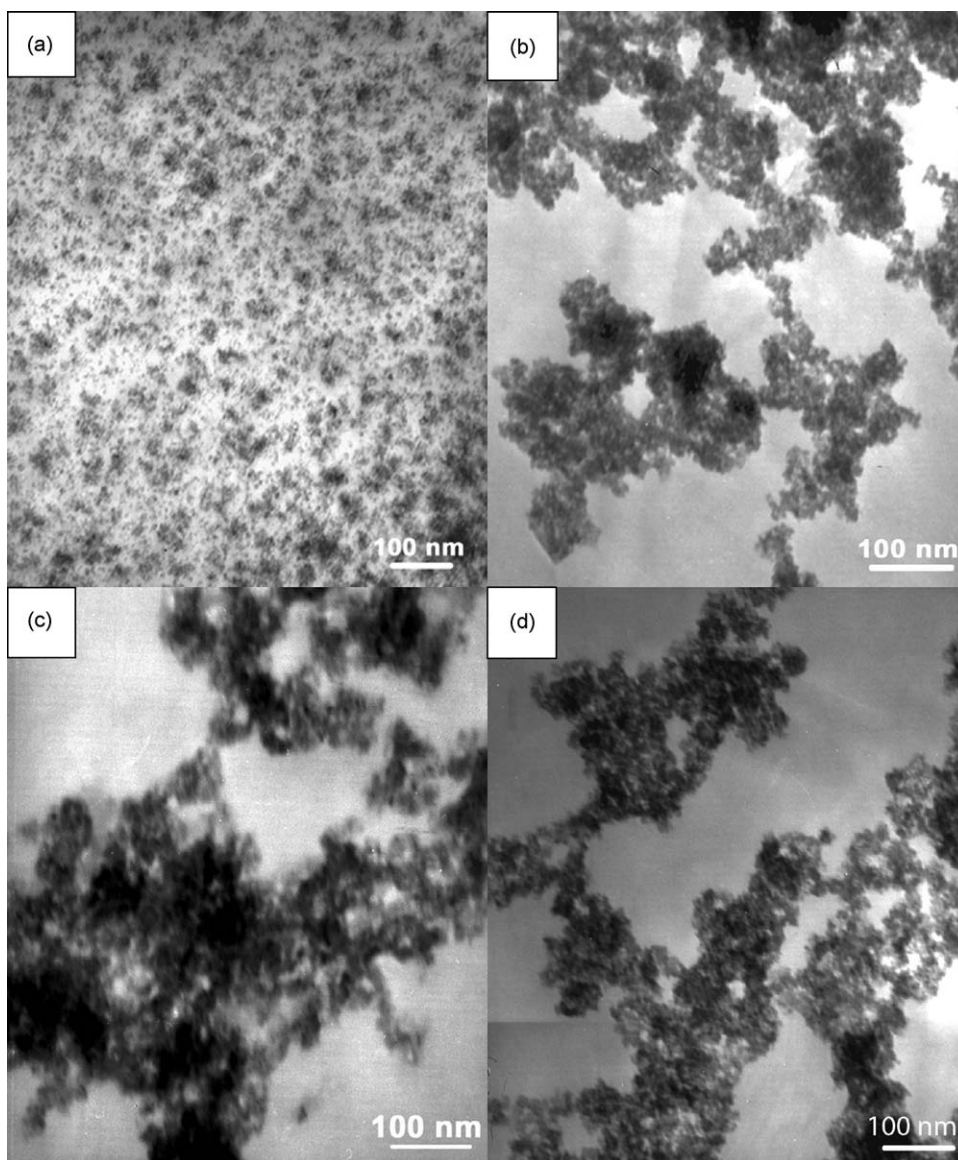
Fig. 2. Typical TEM of TiO$_2$ (a), TTi0.2 (b), TTi0.5 (c) and XTi0.5 (d).

3.3. Surface structure and composition

The FT-IR spectra of the original materials (TiO$_2$, TDI and m-XDI), TTi samples and XTi samples were shown in Figs. 3 and 4. The typical absorption at 2278 cm^{-1} of –NCO groups could be observed only for the TDI and m-XDI themselves (see Figs. 3 and 4). The strong peak at 3441 cm^{-1} of the unmodified TiO$_2$ was attributed to the hydroxyl groups of Ti–OH resulting from the physically absorbed water molecules via weak hydrogen bonds [42]. After the TiO$_2$ was modified by TDI or m-XDI molecules, the band at 2278 cm^{-1} of –NCO groups disappeared and several new absorptions were observed for the TTi and XTi samples (see Figs. 3 and 4). The disappearance of the peak at 2278 cm^{-1} implied that the active –NCO groups reacted completely and no adsorbed/unreacted isocyanate existed in the final products. The new absorptions at 1535 and 1311 cm^{-1} in Fig. 3 and 1537 and 1317 cm^{-1} in Fig. 4, were both attributed to the deformation vibration of N–H and the stretching vibration of N–C, respectively. It was notable that there was great difference in the location of other newly emerged absorption between TTi and XTi samples. For TTi samples, the
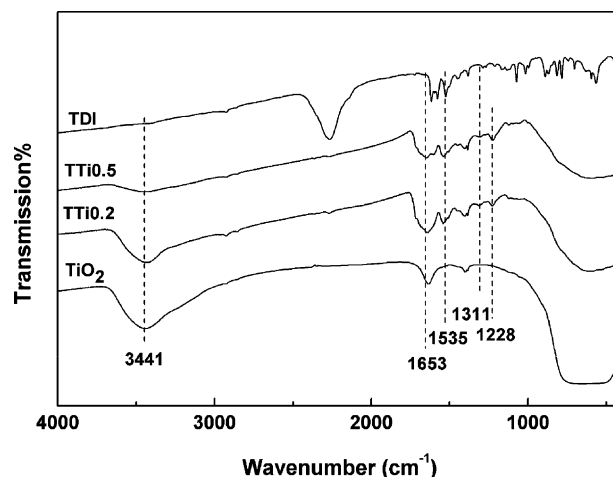

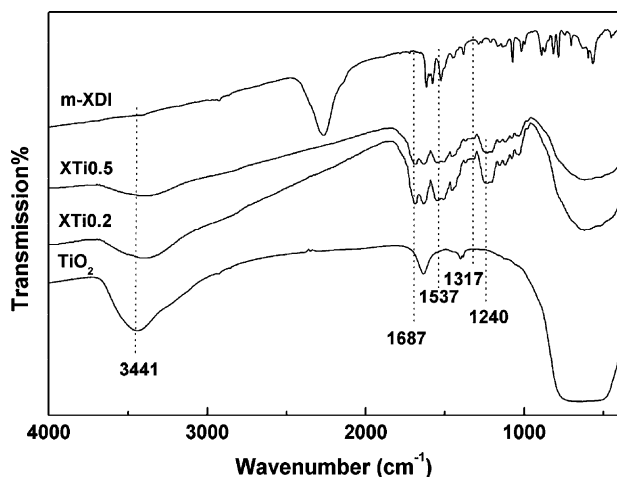**Fig. 3.** FT-IR transmission spectra of TDI, TiO$_2$ and TDI-modified TiO$_2$ samples.

**Fig. 4.** FT-IR transmission spectra of m-XDI, TiO$_2$ and m-XDI-modified TiO$_2$ samples.

newly produced bands at 1653 and 1228 cm^{-1} (see Fig. 3) could be ascribed to the asymmetric stretching vibration and the symmetric stretching vibration of –COOTi, respectively [35]. Compared with the referenced FT-IR data of vibration of –COOTi (1720 and 1270 cm^{-1}) [43], a large shift toward lower wavenumber was due to the formation of the excellent π-conjugated structure Ph–NHCOOTi (see Scheme 1). For XTi samples, the new absorptions located at 1687 and 1240 cm^{-1} (see Fig. 4) were also assigned to the asymmetric stretching vibration and the symmetric stretching vibration of –COOTi, respectively. But there took place a smaller shift between 1687 and 1240 cm^{-1} and the reported results, which should be attributed to the poor π-conjugated structure PhCH$_2$–NHCOOTi (see Scheme 1). According to the FT-IR results, it was concluded that the confirmed structures by FT-IR were consistent with those in Scheme 1, suggesting as-expected reactions had occurred for isocyanate-modified TiO$_2$.

To further prove the structure of isocyanate-modified TiO$_2$ materials, the X-ray photoelectron spectroscopy (XPS) as a surface characterization technique was also employed to characterize these samples. Table 2 showed the detailed surface element content calculated from the survey XPS analysis. It was found only Ti and O element existed on the surface of unmodified TiO$_2$. But for TTi and XTi samples, N and C elements were also detected beside Ti and O elements. Based on above-mentioned FT-IR results, no adsorbed/unreacted TDI molecules existed in the final isocyanate-modified TiO$_2$ samples. Therefore, the newly emerged N and C elements for TTi and XTi samples should only resulted from the isocyanate molecules (C$_9$H$_6$N$_2$O$_2$ or C$_{10}$H$_8$N$_2$O$_2$) anchored on the TiO$_2$ surface. Moreover, with the increasing content of isocyanate, the N and C amounts obviously increased and the Ti and O content all decreased. The increased isocyanate usage could lead to high surface coverage of isocyanate to TiO$_2$. Considering the measured scope of XPS was fixed, it was reasonable that the higher the entire surface coverage was, the less Ti and O elements could be detected and reversely the higher N and C contents.
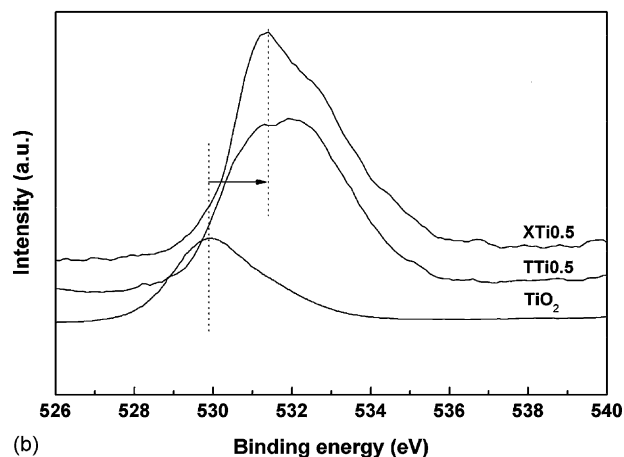
Table 2
The surface element content of samples calculated from XPS analysis.

Samples	Ti 2p %	O 1s %	N 1s %	C 1s %
TiO$_2$	37.96	62.04	/	/
TTi0.2	7.05	26.00	5.44	61.51
TTi0.5	3.11	25.84	6.77	64.28
XTi0.2	7.54	27.09	4.84	60.53
XTi0.5	3.26	26.89	5.95	63.90
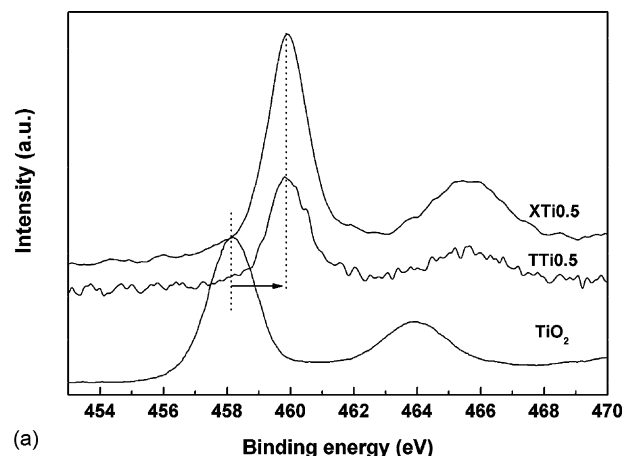
Fig. 5. High-resolution XPS spectra in the Ti 2p region (a) and the O 1s region (b) for the TiO$_2$, TTi0.5 and XTi0.5 samples.

Fig. 5 exhibited the high-resolution XPS spectra of TiO$_2$, TTi0.5 and XTi0.5. Compared with the spectra of unmodified TiO$_2$, an obvious shift to higher binding energies could be observed in both the Ti 2p region and the O 1s region of TTi and XTi samples, which was the result of the chemical interaction between TiO$_2$ and isocyanate molecules. The increased binding energies of isocyanate-modified TiO$_2$ samples were also good evidences for surface modification to TiO$_2$ by chemical bonds not by adsorption. The high-resolution spectra of C 1s region, presented in Fig. 6, were decomposed into three contributions, including C–C or C=C groups in aromatic rings, C=O groups, C–O or C–N groups [44]. Because the detected C element only came from those anchored isocyanate molecules (TDI or XDI) on the TiO$_2$ surface, these three contributions in C1s XPS spectra were very powerful evidences to confirm the surface chemical structure of isocyanate-modified TiO$_2$ samples. Additionally, the XPS results were in good agreement with the FT-IR results and further prove the structure of TDI-modified TiO$_2$ predicted in Scheme 1.

3.4. UV–Vis absorption

According to the former structure analysis of isocyanate-modified TiO$_2$ in Section 3.1, theoretically, the isocyanate modification to TiO$_2$ can improve its UV–Vis absorption. Fig. 7 showed the UV–Vis diffuse reflectance spectra of unmodified TiO$_2$, TTi and XTi samples. The inset showed the UV–Vis spectra of TDI and m-XDI without any absorption above 400 nm. Seen from Fig. 7, the unmodified TiO$_2$ showed very weak visible absorption, but the
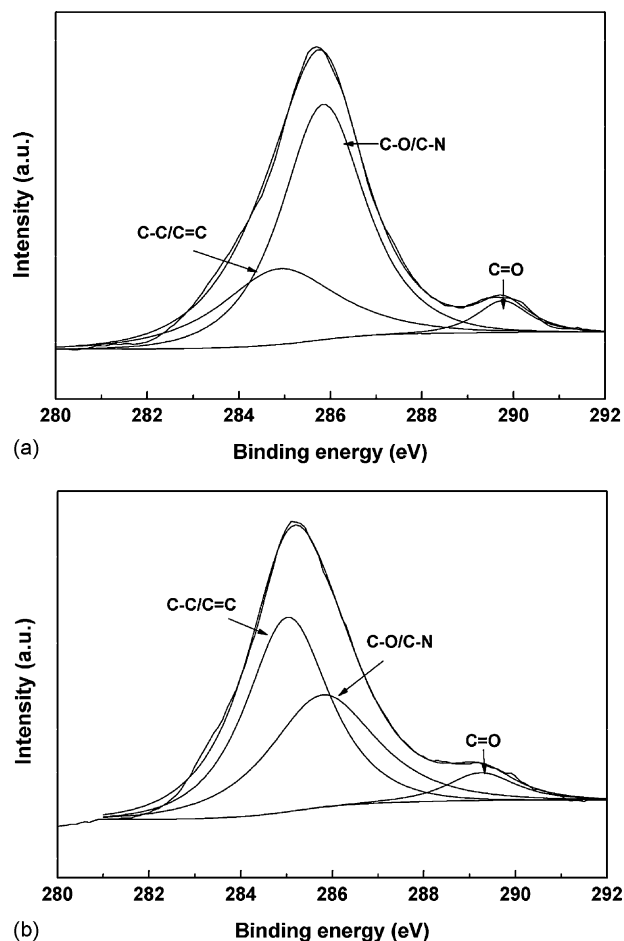
Fig. 6. Fit to the C 1s region of the XPS spectra for TTi0.5 (a) and XTi0.5 (b).

the rise of TDI or m-XDI content. Noticeably, TTi samples had stronger visible absorption than XTi samples (see Fig. 7) with the same molecular ratio of isocyanate/TiO2. To explain this phenomenon, the structure of isocyanate-modified TiO2 was necessary to be discussed because the absorptive property was mainly decided by the chemical structure. Seen from Scheme 1, the structures of TTi and XTi samples were of typical donor–acceptor type π-conjugated structure, where the π-conjugated surface complexes was electron donor and Ti was electron acceptor due to its electron-deficient of d-orbital. These donor–acceptor type chemical structures led to the extension of π-conjugation via the electron-deficient d-orbital and finally to the decrease of the electron-transition energy [45–47]. Consequently, the electrons in donor–acceptor type π-conjugated system may easily transfer from organic part to inorganic part (ligand-to-metal), resulting in the red-shift in the UV–Vis absorption. For TTi samples, the electron donor was more perfect π-conjugated structured surface complexes because TDI molecule was conjugated itself. The obtained TTi samples possessed a bigger donor–acceptor type conjugated system, which could lead to lower electron-transition energy. Therefore, the TTi samples showed stronger visible absorption. But the electron donor in XTi samples was only the π-conjugated bonds (–NHCOO–) not the whole surface complexes due to the lack of conjugation of XDI molecules. As the result, the XTi samples with incomplete donor–acceptor type conjugated structure, showed weaker visible absorption than TTi samples.

3.5. Photocatalytic studies

The isocyanate-modified TiO2 showed obvious visible response due to the formation of π-conjugated surface complexes on TiO2 surface, and that the surface complexes could enhance the electron-transfer rates of TiO2 [35,36,48]. Therefore, the isocyanate-modified TiO2 catalysts may exhibit improved visible photocatalytic activity compared with unmodified TiO2. For comparison, two blank experiments were carried out, including one under visible irradiation without catalysts and another in the dark with catalysts. Both of them showed no MB degradation.

The photocatalytic results for the degradation of MB were shown in Fig. 8. Seen from Fig. 8, unmodified TiO2 had very poor photocatalytic activity, and isocyanate-modified TiO2 samples showed largely enhanced activity compared with unmodified TiO2. The improved photocatalytic activity of isocyanate-modified TiO2 catalysts should be attributed to the enhanced visible absorption

visible absorption of TTi and XTi samples was improved. Especially, TTi0.5 showed very obvious visible absorption (see Fig. 7). Compared with the original materials (TiO2, TDI and m-XDI), the isocyanate-modified TiO2 samples showed a red-shift in UV–Vis absorption, which could be attributed to the intramolecular ligand-to-metal charge transfer transition [35,36]. Moreover, the intensity of visible absorption for TTi or XTi samples increased with
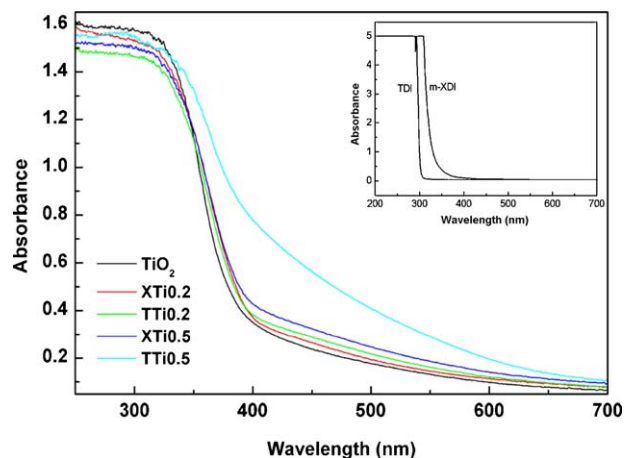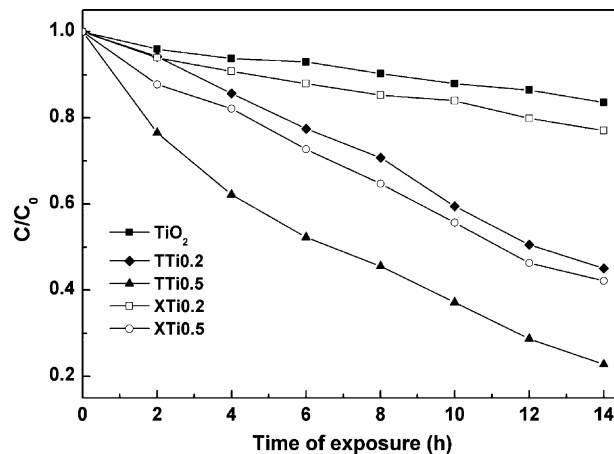

Fig. 7. UV–Vis diffuses reflectance spectra of TiO2 and isocyanate-modified TiO2 samples. The inset gives the UV–Vis spectra of TDI and m-XDI.

Fig. 8. Photocatalytic degradation of MB under visible light in catalysts suspension at natural PH, [catalyst] = 1 g L^{-1}, [MB]$_0$ = 50 ppm (the absorption spectra were recorded after 4-fold dilution).

and the increasing electron-transfer rates due to the surface complexes. Moreover, the photocatalytic activity of isocyanate-modified TiO_2 samples increased with the increase of isocyanate/TiO_2 molar ratio. Especially, TTi0.5 displayed the highest visible photocatalytic activity due to the strongest absorption in visible region (see Fig. 7). It should be noticed that XTi samples exhibited much weaker photocatalytic activity than TTi samples when the dosage of isocyanate to modify TiO_2 was identical. This difference should mainly ascribe to the different intensity of visible absorption between TTi and XTi samples. Essentially, the different photocatalytic activity was on account of the difference in their structure. According to the above analysis, under the same reaction condition, the better the conjugated structure the isocyanate-modified TiO_2 samples had, the higher photocatalytic activity the as-prepared catalysts showed.

Noticeably, since MB could absorb visible light itself, it could inevitably act as a sensitizer for TiO_2. Generally, it was necessary to the aim of photocatalytic sensitization that MB must adsorb on TiO_2 surface. Moreover, the larger the adsorption amount was, the stronger the sensitization effect of MB to TiO_2 was. For unmodified TiO_2, it could show visible photocatalytic activity due to the MB sensitization. But, for isocyanate-modified TiO_2, because the TiO_2 surface was covered by the isocyanate molecules, the amount of MB directly contacting with TiO_2 decreased with the enhanced isocyanate modification. Thus the MB sensitization effect to TiO_2 was greatly weakened for isocyanate-modified TiO_2. As a result, the obviously improved visible photocatalytic activity of isocyanate-modified TiO_2 should not be attributed to the sensitization effect of MB to TiO_2. The detailed photocatalytic mechanism would be discussed later.

3.6. Stability of catalysts

To investigate the stability of catalyst, TTi0.5 as a representative photocatalyst, was tested under 24-h visible light irradiation in aqueous suspension without MB. It was found that no noticeable change was observed in the UV–Vis diffuse reflectance spectra and FT-IR spectra of TTi0.5 before and after visible light irradiation (see Figure S1 and S2 in supporting information), which indicated TTi0.5 was very photostable. In addition, a recycled photocatalytic examination of TTi0.5 was also carried out, and the corresponding result was given in Fig. 9. It was found that twice-recycled TTi0.5 catalyst still exhibited good photocatalytic activity. Based on the above results, the TTi0.5 catalyst was photostable.
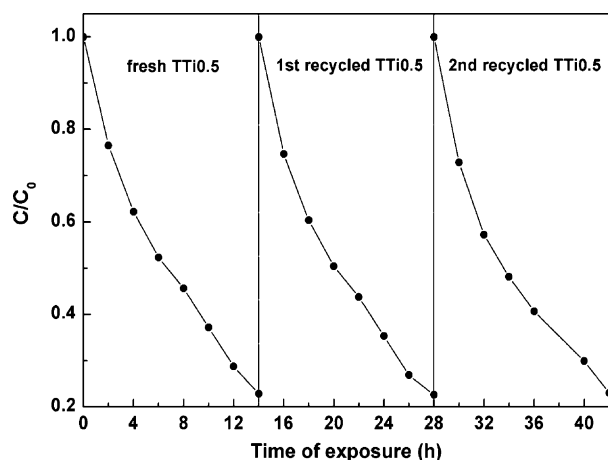
3.7. Mechanism of photocatalysis

MB can undergo photodegradation under visible irradiation in aqueous TiO_2 suspension, which not only led to photobleaching but also causes a complete decomposition of MB to evolve CO_2 [49,50]. The photodegradation pathway under visible irradiation is different from that under UV light in TiO_2 suspension. Herein, the mechanism of the photocatalytic decomposition of MB over isocyanate-modified TiO_2 under visible light was also discussed. There may be two routes to realize the photocatalytic degradation for our as-prepared isocyanate-modified TiO_2, including the process (1) and (2) (see Fig. 10). In the process (1), the modification of isocyanate to TiO_2 led to form surface complexes on the TiO_2 surface. The surface complexes could absorb visible light and then were excited by visible light followed by electron injection into the conduction band of TiO_2. As a result, the surface complex became cationic radical. Simultaneously, the MB molecules absorbed on the surface complex could transfer electrons into the cationic radical of surface complex and generated $MB^{\bullet+}$. $MB^{\bullet+}$ was essential to further photocatalytic reaction. Those electrons of TiO_2 conduction band was scavenged by the O_2 preadsorbed on the TiO_2 surface to form superoxide anion radical ($O_2^{\bullet-}$), which further converted to hydrogen peroxide radicals ($HOO^\bullet$) and hydroxyl radicals ($HO^\bullet$) via a series of protonation, disproportionation and reduction steps. In addition to the above process (1), the photocatalytic degradation could still be realized as the process (2). According to the previous analysis, it was known that MB was adsorbed on the surface complexes not on TiO_2. So, there was possible that MB could have sensitization effect on the isocyanate-modified TiO_2. When MB absorbed the visible light and was excited into MB^*, MB^* could transfer an electron to the surface complexes formed by isocyanate modification to TiO_2, and finally generate $MB^{\bullet+}$. Subsequently, the surface complexes injected the accepted electron into the conduction band of TiO_2, and then this electron would give rise of hydroxyl radicals ($HO^\bullet$) according to the same reaction process as shown in process (1). The hydroxyl radicals were proposed to be the primary oxidant in the photocatalytic system. The hydroxyl radicals reacted with the $MB^{\bullet+}$ molecules to generate some intermediates and finally produced the degradation product [51].

Fig. 9. Photocatalytic degradation of MB (50 ppm) with recycled TTi0.5, [catalyst] = 1 g L^{-1}, $[MB]_0$ = 50 ppm.

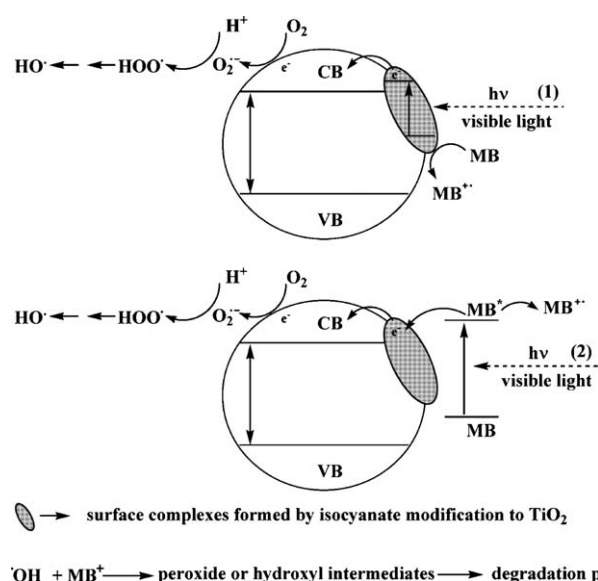**Fig. 10.** The mechanism of the photocatalytic degradation of MB over isocyanate-modified TiO_2 under visible light irradiation.

4. Conclusions

A kind of visible responsible photocatalysts were prepared by isocyanate modification to TiO_2. After TiO_2 modified by isocyanate, π-conjugated surface complexes were produced on the TiO_2 surface by the chemical bonds –NHCOOTi between TiO_2 and isocyanate. Due to the formation of the π-conjugated surface complexes, the obtained isocyanate-modified TiO_2 catalysts showed obvious visible absorption. In addition, different structured isocyanate (conjugated and unconjugated) had different effects on the property of isocyanate-modified TiO_2. Conjugated structured TDI modification to TiO_2 catalysts could produce perfect π-conjugated TTi samples to show stronger visible absorption and better photocatalytic activity than the unconjugated m-XDI.

Acknowledgement

Appendix A. Supplementary data

Supplementary data associated with this article can be found, in the online version, at doi:10.1016/j.apcatb.2008.09.021.

References

[1] A. Fujishima, K. Honda, Nature 238 (1972) 37–38.
[2] Z.S. Wang, F.Y. Li, C.H. Huang, L. Wang, M. Wei, L.P. Jin, N.Q. Li, J. Phys. Chem. B 104 (2000) 9676–9682.
[3] J. Aguado, R. van Grieken, M.J. López-Muñoz, J. Marugán, Catal. Today 75 (2002) 95–102.
[4] J. Zhou, M. Takeuchi, A.K. Ray, M. Anpo, X.S. Zhao, J. Colloid Interface Sci. 311 (2007) 497–501.
[5] H. Kisch, L. Zang, C. Lange, W.F. Maier, C. Antonius, D. Meissner, Angew. Chem. Int. Ed. 37 (1998) 3034–3036.
[6] L. Zang, C. Lange, I. Abraham, S. Storck, W.F. Maier, H. Kisch, J. Phys. Chem. B 102 (1998) 10765–10771.
[7] H. Yamashita, Y. Ichihashi, M. Takeuchi, S. Kishiguchi, M. Anpo, J. Synchrotron Radiat. 6 (1999) 451–453.
[8] M. Anpo, M. Takeuchi, Int. J. Photoenergy 3 (2001) 89–94.
[9] L. Zang, W. Macyk, C. Lange, W.F. Maier, C. Antonius, D. Meissner, H. Kisch, Chem. Eur. J. 6 (2000) 379–384.
[10] H. Yamashita, M. Harada, J. Misaka, M. Takeuchi, B. Neppolian, M. Anpo, Catal. Today 84 (2003) 191–196.
[11] M. Iwasaki, M. Hara, H. Kawada, H. Tada, S. Ito, J. Colloid Interface Sci. 224 (2000) 202–204.
[12] W. Macyk, H. Kisch, Chem. Eur. J. 7 (2001) 1862–1867.
[13] G. Burgeth, H. Kisch, Coord. Chem. Rev. 230 (2002) 41–47.
[14] S. Khan, M. Al-Shahry, W.B. Ingler, Science 297 (2002) 2243–2245.
[15] C. Lettmann, K. Hildenbrand, H. Kisch, W. Macyk, W.F. Maier, Appl. Catal. B: Environ. 32 (2001) 215–227.
[16] R. Asahi, T. Morikawa, T. Ohwaki, A. Aoki, Y. Taga, Science 293 (2001) 269–271.
[17] Y. Kuroda, T. Mori, K. Yagi, N. Makihata, Y. Kawahara, Y. Nagao, S. Kittaka, Langmuir 21 (2005) 8026–8034.
[18] H. Irie, Y. Watanabe, K. Hashimoto, J. Phys. Chem. B 107 (2003) 5483–5846.
[19] C. Burda, Y.B. Lou, X.B. Chen, A.C.S. Samia, J. Stout, J.L. Gole, Nano Lett. 3 (2003) 1049–1051.
[20] H. Fu, L. Zhang, S. Zhang, Y. Zhu, J. Zhao, J. Phys. Chem. B 110 (2006) 3061–3065.
[21] X. Chen, Y. Lou, A.C.S. Samia, C. Burda, J.L. Gole, Adv. Funct. Mater. 15 (2005) 41–49.
[22] J.L. Gole, J.D. Stout, C. Burda, Y. Lou, X. Chen, J. Phys. Chem. B 108 (2004) 1230–1240.
[23] A. Ghicov, J.M. Macak, H. Tsuchiya, J. Kunze, V. Haeublein, L. Frey, P. Schmuki, Nano Lett. 6 (2006) 1080–1082.
[24] O. Diwald, T.L. Thompson, T. Zubkov, E.G. Goralski, S.D. Walck, J.T.Y. Jr, J. Phys. Chem. B 108 (2004) 6004–6008.
[25] T. Umebayashi, T. Yamaki, H. Itoh, K. Asai, Appl. Phys. Lett. 81 (2002) 454–456.
[26] D.B. Hamal, K.J. Klabunde, J. Colloid Interface Sci. 311 (2007) 514–522.
[27] J. Wang, S. Yin, Q. Zhang, F. Saito, T. Sato, Chem. Lett. 32 (2003) 540–541.
[28] W. Zhao, W. Ma, C. Chen, J. Zhao, Z. Shuai, J. Am. Chem. Soc. 126 (2004) 4782–4783.
[31] J. Moon, C. Yun, K. Chung, M. Kang, J. Yi, Catal. Today 87 (2003) 77–86.
[32] D. Chatterjee, A. Mahata, Appl. Catal. B: Environ. 33 (2001) 119–125.
[33] M.R. Hoffmann, S.T. Martin, W. Choi, D.W. Bahnemannt, Chem. Rev. 95 (1995) 69–96.
[34] Y. Liu, J.I. Dadap, D. Zimdars, K.B. Eisenthal, J. Phys. Chem. B 103 (1999) 2480–2486.
[35] J. Moser, S. Punchihewa, P.P. Infelta, M. Grätzel, Langmuir 7 (1991) 3012–3018.
[36] A.E. Regazzoni, P. Mandelbaum, M. Matsuyoshi, S. Schiller, S.A. Bilmes, M.A. Blesa, Langmuir 14 (1998) 868–874.
[37] S. Ikeda, C. Abe, T. Torimoto, B. Ohtani, J. Photochem. Photobiol. A: Chem. 160 (2003) 61–67.
[38] D. Jiang, Y. Xu, B. Hou, D. Wu, Y. Sun, J. Solid State Chem. 180 (2007) 1787–1791.
[39] D. Jiang, Y. Xu, D. Wu, Y. Sun, J. Solid State Chem. 181 (2008) 593–602.
[40] Z. Li, B. Hou, Y. Xu, D. Wu, Y. Sun, W. Hu, F. Deng, J. Solid State Chem. 178 (2005) 1395–1405.
[41] R. Rodríguez, M.A. Blesa, A.E. Regazzoni, J. Colloid Interface Sci. 177 (1996) 122–131.
[42] T. Bezrodna, G. Puchkovska, V. Shimanovska, I. Chashecnikova, T. Khalyavka, J. Baran, Appl. Surf. Sci. 214 (2003) 222–231.
[43] S. Doeuff, M. Henry, C. Sanchez, J. Livage, J. Non-Cryst. Solids 89 (1987) 206–216.
[44] S. Biniak, G. Szymanskj, J. Siedlewskj, A. Swiatkowski, Carbon 35 (1997) 1799–1810.
[45] N. Matsumi, Y. Chujo, O. Lavastre, P.H. Dixneuf, Organometallics 20 (2001) 2426–2427.
[46] B.S. Lele, A.J. Russell, Biomacromolecules 5 (2004) 1947–1955.
[47] N. Matsumi, Y. Chujo, Macromolecules 33 (2000) 8146–8148.
[48] T. Rajh, J.M. Nedeljkovic, L.X. Chen, O. Poluektov, M.C. Thurnauer, J. Phys. Chem. B 103 (1999) 3515–3519.
[49] I. Zhao, K. Wu, H. Hidaka, N. Serpone, J. Chem. Soc. Faraday Trans. 94 (1998) 673–676.
[50] F. Zhang, J. Zhao, L. Zang, T. Shen, H. Hidaka, E. Pelizzetti, N. Serpone, Appl. Catal. B: Environ. 15 (1998) 147–156.
[51] T. Wu, T. Lin, J. Zhao, H. Hidaka, N. Serpone, Environ. Sci. Techonol. 33 (1999) 1379–1387.